

# Land cover change analysis in Majalengka Regency using the pan-sharpening method and random forest machine learning algorithm

Hari Prayogi\*<sup>1</sup>, Hafid Setiadi\*\*, Supriatna\*\*, Dewany\*\*\*

\* Universitas Indonesia, Margonda Raya Street, Pondok Cina, Depok City, West Java, Indonesia and National Research and Innovation Agency, M.H. Thamrin Street No. 8, Jakarta, 10340, Indonesia

\*\* Universitas Indonesia, Margonda Raya Street, Pondok Cina, Depok City, West Java, Indonesia

\*\*\* National Research and Innovation Agency, M.H. Thamrin Street No. 8, Jakarta, 10340, Indonesia

<sup>1</sup>Corresponding author, Email: hari038@brin.go.id

Paper received: 28-03-2023; revised: 10-05-2023; accepted: 17-05-2023

## Abstract

The ever-increasing population has accelerated the need for housing and supporting facilities. Further, this growing number of residences and life support facilities resulted in changes in land cover. For instance, the construction of the West Java International Airport and the increase in the population resulted in land cover changes in Majalengka Regency, Indonesia. This study aims to analyze changes in land cover during 2014, 2018, and 2022 in the Majalengka district using Landsat 8 satellite imagery. We used the pan-sharpening research method, while for the closure classification, we used machine-learning random forest algorithms on the google earth engine platform. The land cover classification classes adopted in this study were natural vegetation, cultivated vegetation, open land, built-up land, and bodies of water. The obtained land cover classification results suggested overall accuracy values of 0.96, 0.94, and 0.93 in 2014, 2018, and 2022 respectively, with kappa index values of 0.950, 0.925, and 0.91667. The results indicate a trend of changes in the land cover in the Majalengka district. From 2014-2022, the trend of increasing land cover area was observed in open land and built-up land, while the decreasing land cover area was found in natural vegetation and cultivated vegetation areas. Using both the pan-sharpening method and the machine learning random forest algorithm, we established images with a more detailed appearance with an outstanding kappa accuracy value (above 0.85). Therefore, the developed algorithm can be used in land cover change mapping analysis.

**Keywords:** land cover changes; pan-sharpening; random forest

## 1. Introduction

In Indonesia, its population is growing annually, while West Java is the most populated province in Indonesia, with a total population of 48,274,162 in 2020 (Central Bureau of Statistics, 2020). With this rapidly increasing population, there are also expanding needs for living facilities. One of the most vital living facilities for human beings is residence. Accordingly, the growing number of population also escalates the number of housing, along with its supporting infrastructures, such as the general and social facilities. Those occurrences induce a change in land usage. Additionally, this transition in land utilization is also caused by other factors, including physical, biological, economic considerations, and institutional factors (Tambajong, Mononimbar, & Lahamendu, 2017).

Examples of institutional factors are the regional regulations and policies related to land cover transformation. The Provincial Government of West Java enacted the West Java Regional

Regulation No 13 in the Year 2010 concerning the establishment and development of West Java International Airports and Kertajati Aerocity. Besides, West Java also has West Java Regional Policy No. 22, the Year 2010, on the West Java Province Regional Spatial Plan for 2009-2029. Following the enactment of Regional Laws No. 11, the Year 2011, about the Majalengka Regency Regional Spatial Plan for 2011-2013, Majalengka was selected as the location of the West Java International Airport construction. Consequently, the manufacturing of international airports impacts the progression of other sectors, such as the upsurge of housing (Andriany & Chofyan, 2016) and other living facilities, provoking a change in land cover. One of the available alternatives for mapping these land-cover changes is the manual or automatic remote sensing satellite imagery interpretation techniques (Fariz, Daeni, & Sultan, 2021). Further, remote sensing also offers the most recent information on the land cover through the land cover map (Sampurno & Thoriq, 2016).

In addition, remote sensing can also facilitate supervision and observation of the changes in the earth's surface since it has extensive area coverage, high temporal resolution, and wide data availability (Zurqani, Post, Mikhailova, Ozalas, & Allen, 2019). It can also be used in vegetation analysis (Marlina, 2022), as well as in observing coral reefs, temperature, and land cover (Fikri, Setiawan, Violando, Muttaqin, & Rahmawan, 2021). Further, there are various data processing techniques for managing remote sensing data, one of them is the pan-sharpening technique (Fari, 2017). Pan-sharpening is defined as an accelerating spatial satellite image by combining multispectral and panchromatic images. This method aims to enhance the spatial information offered by multispectral images by integrating the images with a higher spectral resolution, producing data with better and maximum quality (Hidayati, Susanti, & Utami, 2017). The obtained image from the pan-sharpening method provides more accurate and reliable information as the decision making process, such as in the land-cover classification (Li & Cheng, 2019).

The development of the remote sensing technique is characterized by cloud-based image processing, in which the hard disk storage media is no longer used as it is not flexible and gives limited satellite image processing (Prayogo, 2021). The rapid progression of the technology enables quicker remote sensing data processing using the Google Earth Engine platform (GEE). GEE offers numerous advantages, such as during the coordinate transformation, projection, atmosphere correction, and pixel conversion processes which commonly require extensive storage devices and computers with advanced specifications. The GEE platform reduces the time necessary in the pre-processing stage (Amini, Saber, Rabiei-Dastjerdi, & Homayouni, 2022). Besides, the GEE also appears as an alternative for land cover mapping in expanded areas (Fariz et al., 2021). GEE also serves some machine learning algorithms for data processing and classification of remote sensing satellite image data, such as CART (Classification and Regression Trees), Naïve Bayes, SVM (Support Vector Machine), and Random Forest (Google Developers, 2021).

In this study, we used a random forest machine learning algorithm in processing and classifying remote sensing satellite image data. This algorithm was selected due to its superiorities, namely non-parametric in nature, can be applied to sustainable and categorical sets of data, and is sensitive toward overfitting (Horning, 2010). Additionally, random forest is a learning algorithm based on ensemble learning from a decision tree that contains several gigantic decision trees. The individual bootstrap sample is taken from a set of original data with substitution sampling (Santoso, Tani, & Wang, 2017). This algorithm has been commonly

adopted in the processing and classification of satellite image data, aerial photos, and field data collection (Horning, 2010).

The Gram-Schmidt pan-sharpening method has been used in a study carried out by Hidayati et al. (2017) with Quickbird satellite image, along with the Brovey transformation method, to facilitate visual analysis of the excellent scale land usage classification in Indonesia. Meanwhile, Pradipta, Widyantara, and Hartati (2019) apply the Brovey transformation method using the Landsat 8 image data to combine the quality of Landsat 8 image data with the true color combination, before and after the image sharpening, by calculating the minimum and maximum band red, green, and blue values, as well as analyzing the mean and standard deviation. Another study carried out by Putra and Setiawan (2021) also used the pan-sharpening method on the combination of ALOS AVNIR-2 and PRISM satellite images through the Hue Saturation Value (HSV) method to examine the accuracy of fusion image results and analyzing the land usage in the South Bali, Indonesia. Random forest research conducted by Marlina (2022) also utilized the images from Sentinel 2, the NDVI index method, and the random forest algorithm to analyze the classification of land cover in Kuningan Regency, Indonesia. Zulfajri, Danoedoro, and Murti (2021) also reported the classification of land cover in some areas of Pidie Jaya Regency, Indonesia, using random forest research with the OLI Landsat satellite image data and random forest algorithm method.

As previous studies mainly combined the usage of the pan-sharpening method with the random forest algorithm, we also used those methods in this study. The combination of the pan-sharpening method with the random forest algorithm offers higher quality and more detailed Landsat 8 satellite images with 15 meters of spatial resolution. Thus, with these methods, we have a better land cover classification in the Majalengka Regency, Indonesia. Accordingly, this study aims to analyze the change in land cover trend in Majalengka Regency, Indonesia, in 2014, 2018, and 2022 using pan-sharpening and machine learning random forest algorithms. The results of this study are expected to be a reference for future decision-making or policy enactment and studies related to land cover, particularly in Majalengka Regency, Indonesia.

## **2. Method**

### **2.1. Research Location**

This study was carried out in the administrative area of Majalengka Regency, West Java Province, Indonesia, at 108°03' EL - 108°25' EL dan 6°36' SL - 7°44' SL, as illustrated in Figure 1. From its geographical condition, the area of Majalengka Regency can be divided into three zones, namely the mountainous region with 500-857 m above sea level of height, undulating or hilly areas with a height of 50-500 m above sea level, and the lowland area with the height of 19-50 m above the sea level (The Ministry of Communication and Informatics of Majalengka, 2023). Its lowland area and its position connecting four regencies in West Java (Sumedang, Indramayu, Cirebon, and Kuningan Regencies) positioned Majalengka Regency as a potential business and industrial center.

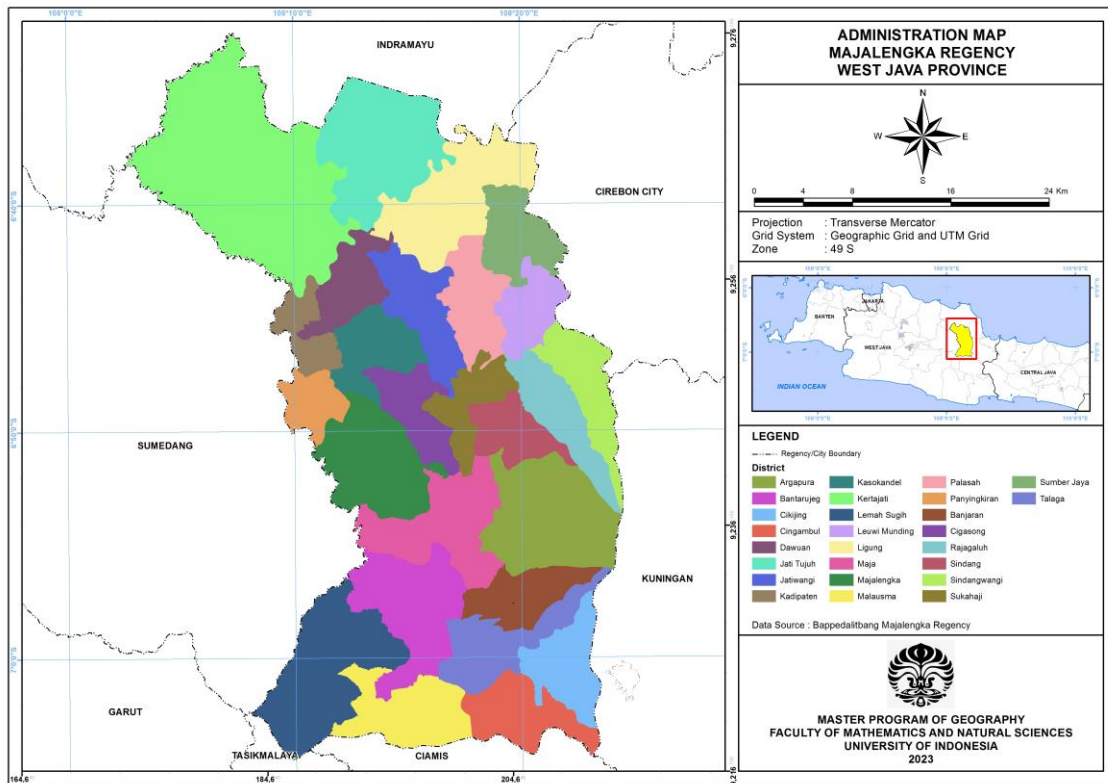


**Figure 1. Research Location**

## 2.2. Material and Instrument

In this study, we used a compilation of mosaic data from Landsat 8 Top of Atmosphere (ToA) level 1 collected from January 1<sup>st</sup> to December 31<sup>st</sup> of 2014, 2018, and 2020 in the Majalengka Regency. Specifically, we used the canal or bands 1, 2, 3, 4, 5, 6, 7, and 8 of the Landsat 8 satellite images from the United Soil Geological Survey (USGS) accessed through the GEE platform. We also added the NDVI, NDBI, and NDWI index to the calculation of the Landsat 8 satellite image to enhance the classification of land cover using the random forest machine learning algorithm. For the administrative border, we used the Spatial Pattern Map from the Regional Development Institution for Research and Development for Majalengka Regency, Indonesia.

In addition, we also used several instruments, such as the Google Earth Engine (GEE) platform, ArcGIS software, Global Positioning System (GPS), camera, and computer hardware. Google Earth Engine was used for data processing from Landsat 8 data images, while ArcGIS was employed in data processing and layout, or GEE image classification and the camera was used for the storage of location data and documentation of land-cover survey.

## 2.3. Landsat 8 Satellite

The Landsat 8 Satellite is one of the generations of Landsat satellites launched on February 11th, 2013, by the United States Geological Survey (USGS) NASA. This Landsat 8 Satellite has an operational land imager (OLI) sensor and thermal infrared sensor (TIRS). The OLI (Operational Land Imager) sensor on Landsat 8 has one near-infrared canal and seven

visible canals with an electromagnetic spectrum range. Besides, all of those canals have 30 meters of spatial resolution. Meanwhile, the thermal sensor and panchromatic canals have a spatial resolution of 100 and 15 meters. In one data recording, the Landsat 8 satellite produces 11 data canals, as summarized in Table 1 (NASA, 2013).

**Table 1. Band Specification on Landsat 8 Satellite's Censors**

No	Band	Wavelength	Spatial Resolution
1	Band 1- Coastal/Aerosol	0.435 – 0.451 $\mu\text{m}$	30 meters
2	Band 2 - Blue	0.452 – 0.512 $\mu\text{m}$	30 meters
3	Band 3 - Green	0.533 – 0.590 $\mu\text{m}$	30 meters
4	Band 4 - Red	0.636 – 0.673 $\mu\text{m}$	30 meters
5	Band 5 - NIR	0.851 – 0.879 $\mu\text{m}$	30 meters
6	Band 6 - SWIR-1	1.566 – 1.651 $\mu\text{m}$	30 meters
7	Band 7 - SWIR-2	2.107 – 2.294 $\mu\text{m}$	30 meters
8	Band 8 - Panchromatic	0.503 – 0.676 $\mu\text{m}$	15 meters
9	Band 9 - Cirrus	1.363 – 1.384 $\mu\text{m}$	30 meters
10	Band 10 - TIRS-1	10.60 -11.19 $\mu\text{m}$	100 meters
11	Band 11 - TIRS-2	11.50 -12.51 $\mu\text{m}$	100 ters

#### 2.4. Data Processing

During the data processing, we combined the data from satellite images (data mosaic), pan sharpening, land cover classification, sample selection, field survey, accuracy test, and the analysis method for land cover analysis. The stages of data processing are illustrated in Figure 2. The data from 2014, 2018, and 2022 (a four-year repeating pattern) were collected for the sources of land cover map construction. Besides, these years were selected due to the establishment of West Java International Airport, which was started in 2014 and operated starting from 2018 (Communication and Public Information Bureau of the Ministry of Transportation, 2018).

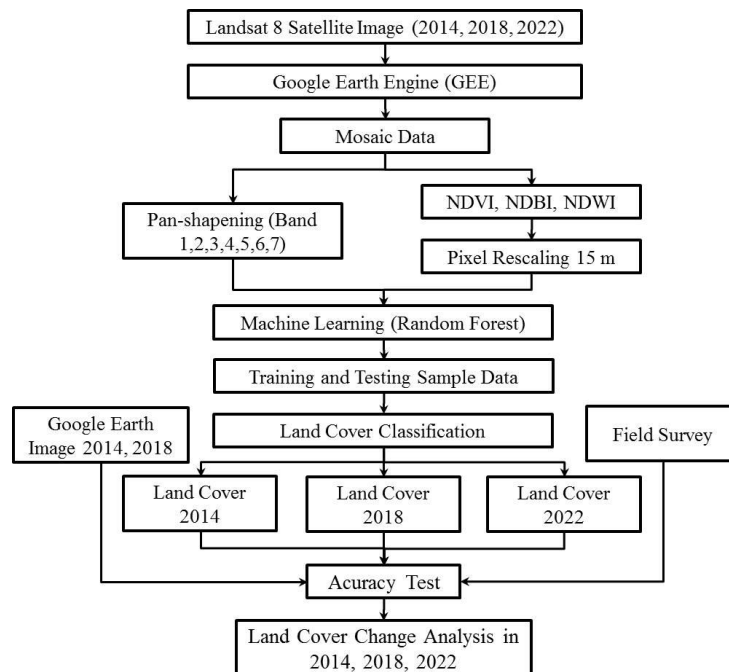


**Figure 2. Research Data Processing**

### 2.4.1. Combination of Satellite Image Data (Mosaic Data)

The mosaic data were obtained from Landsat 8 satellite by removing the cloud cover and cloud shadow. After that, we replaced them with the other Landsat 8 satellite images from the same year using the data masking technique on the GEE platform using a QA band with pixels representing the information related to types of clouds. This masking process is also commonly referred to as the process of removing or deleting clouds on Landsat 8 satellite image data. The disappearance of cloud cover on the combined data or mosaic data from the Landsat 8 satellite generates better land cover classification. Then, the collected Landsat 8 satellite image underwent pan sharpening, while the land cover classification was completed using a random forest machine learning algorithm, followed by an accuracy test and land cover transformation analysis in Majalengka Regency.

### 2.4.2. Pan Sharpening

Pan sharpening is a sharpening combination between the multispectral (30 meters of spatial resolution) and panchromatic (15 meters of spatial resolution) images (Fari, 2017). The variety of multispectral and panchromatic satellite images was first proposed by Dr. Yun Zang, a lecturer in the Geodesy and Geometric Study Program of the University of Brunswick (Putra & Setiawan, 2021). Further, the data produced from the combination of panchromatic and multispectral waves visualized into an image with high spatial resolution facilitates the data processing process in interpreting the land cover data (Hidayati et al., 2017). In this study, we used Hue Saturation Value (HSV) pan-sharpening method.

Through this HSV pan sharpening, we obtained a pan sharpening image with excellent spatial resolution, as illustrated in Figure 3 (Putra & Setiawan, 2021). The pan-sharpening method could be completed on Landsat 8 satellite image through the GEE platform. Further, the attained HSV pan-sharpening images were used as the input data for the land cover classification using the random forest machine learning algorithm.

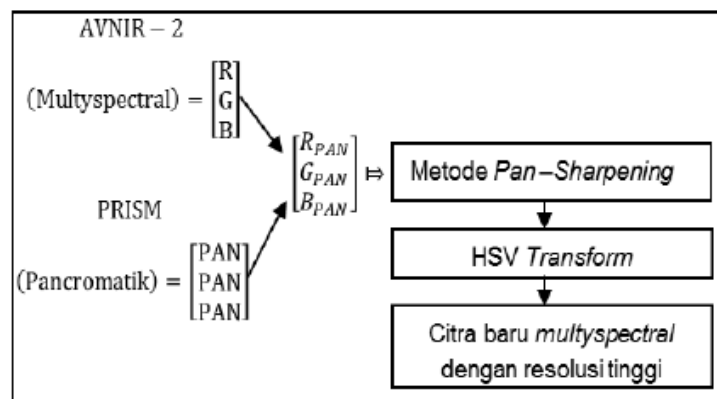


**Figure 3. Image Fusion Algorithm with HSV Method**

### 2.4.3. Land Cover Classification

In this study, we classified the land cover using the random forest machine learning algorithm on the GEE platform. This algorithm facilitates a supervised classification which is essential for the land-cover analysis (Wang, Wang, & Qin, 2021). Meanwhile, the GEE platform

was selected as it aids and accelerates the classification process using the Landsat 8 image data and Google cloud-based data processing. In detail, the random forest machine learning was carried out by inputting the 1 to 7 canals or bands from the Landsat 8 that had undergone the pan sharpening with three indices of NDVI, NDBI, and NDWI. We used the 1 to 7 bands of the Landsat 8 images data as those bands combination offers the most excellent accuracy in comparison to the other band combinations (Fariz et al., 2021). Further, using the NDVI index, we identified the intensity of the vegetation or plant objects, while the NDBI and NDWI indexes were used to examine the intensity of built-up land objects or buildings and water or aquatic objects, respectively. The NDVI (Kshetri, 2018), NDBI (Kshetri, 2018), and NDWI (Nugroho, 2013) calculations used in this study are presented in the following.

$$NDVI = \frac{NIR-RED}{NIR+RED} \quad (1)$$

$$NDBI = \frac{SWIR1-RED}{SWIR1+RED} \quad (2)$$

$$NDWI = \frac{Green-RED}{Green+RED} \quad (3)$$

The obtained NDVI, NDBI, and NDBI index underwent pixel rescaling to 15 meters. This pixel rescaling process was carried out to equalize the pixel resolution of the pan sharpening results (15 meters resolution) and the calculated results based on the authentic band spectral from the Landsat 8 satellite image. All of the attained bands and indexes were used as the input for land cover classification using the random forest machine learning algorithm. The conceptual framework of the random forest machine learning algorithm is illustrated in Figure 4 (Koehrsen, 2017).

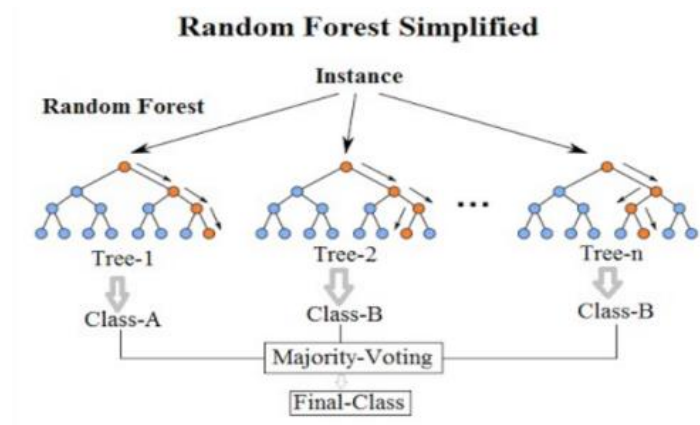


**Figure 4. Simple Conceptual Framework of Random Forest**

Prior to the classification process, the data were divided into two groups, namely the training data (75%) and testing data (25%) (Zulfajri et al., 2021). The land cover classification was carried out referring to the SNI 7645-1-2014, consisting of natural vegetation, cultivated vegetation, open land, built-up land, and water (BSN, 2014).

#### **2.4.4. Sampling and Field Survey**

The sampling was conducted using stratified random sampling with the strata of land cover classification. In the end, we obtained 30 sample points for each stratum of land cover

classification, so the total sample point was 150. The equilibrium between the survey data per class is exceptionally essential to prevent the bias model into specific strata. Besides, we also ensured that each survey point had a minimum of 2 pixels of distance within the Landsat image data after the pan-sharpening process. Further, we have to conduct a ground check on the sample points (Zulfajri et al., 2021).

#### 2.4.5. Test of Accuracy

The accuracy percentage of the obtained mapping was determined based on the results of the accuracy assessment by identifying the error of land cover classification in the research location. The mapping accuracy was investigated through the confusion matrix, as shown in Table 2 (Sampurno & Thoriq, 2016). The accuracy can be measured using user accuracy, producer accuracy, and overall accuracy.

**Table 2. Confusion Matrix**

		Reference Data				Total	<i>User's Accuracy</i>
		A	B	C	D		
Classification Data	A	X <sub>ii</sub>				X <sub>i+</sub>	(X <sub>ii</sub> /X <sub>i+</sub> ) x 100%
	B						
	C						
	D				X <sub>ii</sub>		
Total		X <sub>+i</sub>					
Producer's Accuracy		(X <sub>ii</sub> /X <sub>+i</sub> ) x 100%					

The calculation of the accuracy test results was completed mathematically using the following formulas from Awaliyan and Sulistyoadi (2018), Huang, Chen, Tao, Huang, and Gu (2018), Sampurno and Thoriq (2016).

$$\text{User's Accuracy} = \left(\frac{X_{ii}}{X_{i+}}\right) \times 100\% \quad (4)$$

$$\text{Producer's Accuracy} = \left(\frac{X_{ii}}{X_{+i}}\right) \times 100\% \quad (5)$$

$$\text{Overall Accuracy} = \left(\frac{\sum_i X_{ii}}{N}\right) \times 100\% \quad (6)$$

Description:

N = the total pixel in the example

X = diagonal value from the contingency matrix in the i-line and i-column

X<sub>ii</sub> = the total pixel in the i-line

X<sub>i+</sub> = the total pixel in the i-column

In addition to the overall accuracy, we also calculated the kappa index to discover the accuracy of the obtained land cover classification. The kappa index also considered the error factors during the land cover classification process. Accordingly, the kappa index values should be lower than the obtained overall accuracy since the kappa index regards only the correct data obtained from the classification and field conditions (Wiweka, Prayogo, Marini, & Budiman, 2014).

Mathematically, the kappa index calculation was conducted using the following formula (Sampurno & Thoriq, 2016).

$$K_{hat} = \frac{N \sum_{i=1}^r x_{ii} - \sum_{i=1}^r (x_{i+} + x_{+i})}{N^2 - \sum_{i=1}^r (x_{i+} + x_{+i})} \quad (7)$$

Description:

Khat : the value of kappa accuracy

x+i : total pixel from the i-land usage classification

xi+ : total pixel from the reference of i-land usage

xii : total pixel from the reference of i-land usage following the pixel of the i-land usage classification

i : line of column

r : a total of land usage strata

N : an overall total of pixels from the reference

### 2.5 Analysis of Land Cover Transformation

The analysis of land cover was completed using spatial and tabular analysis. The spatial analysis was carried out by describing the land cover transformation pattern in the Majalengka Regency spatially during 2014, 2018, and 2022. Meanwhile, the tabular analysis was carried out by measuring the area and percentage of land cover changes in each class of land cover based on the obtained classification results from the Landsat 8 image data using the pan-sharpening method and random forest machine learning algorithm in 2014, 2018, and 2022.

## 3. Results and Discussion

### 3.1. Test of Accuracy

The accuracy test on the results of remote sensing image classification was conducted by calculating the overall accuracy and the kappa index. In the calculation, we input the sample points data from two data sources, namely the accuracy test points from the Google Earth satellite images and the test points from the field survey data. The data from Google Earth images were used for measuring the overall accuracy and the kappa index from the classification data obtained from the Landsat 8 satellite images in 2014 and 2018. Meanwhile, the field survey data were utilized in the overall accuracy and kappa index calculation on the classification data from Landsat 8 satellite images in 2022. The results of the land cover classification's accuracy in 2014, 2018, and 2022 are presented in Table 3.

**Table 3. Results of Overall Accuracy and Kappa Index**

No	Year	Overall Accuracy	Kappa Index
1	2014	0,96000	0,95000
2	2018	0,93333	0,91667
3	2022	0,92000	0,90000

The accuracy of the obtained land-cover map in 2014, 2018, and 2022 are summarized in Table 3. The highest accuracy was observed from the land-cover classification in 2014, with overall accuracy and kappa index of 0.96000 and 0.95000, respectively. Meanwhile, the lowest accuracy was on the land cover classification in 2022, with 0.92000 overall accuracies and 0.90000 kappa index. All of the obtained overall accuracy and kappa index are above 0.85 or 85%, showing their excellent accuracy (Bhisma, 1997). This finding suggests that the obtained classification from Landsat 8 satellite images has relatively high accuracy (Marlina, 2022).

Besides, the attained overall accuracy and kappa index have met the requirements from the USGS of higher than 0.85 or 85% interpretation accuracy (Sampurno & Thoriq, 2016).

### 3.2. Land Cover Area in Majalengka Regency

From the data processing, we obtained the area of land cover and its percentage toward the total land cover in Majalengka Regency in 2014, 2018, and 2022. The results are summarized in Table 4.

**Table 4. Changes in Land Cover Area between 2014-2012**

No	Land Cover	Area in 2014 (km <sup>2</sup> )	Percentage (%)	Area in 2018 (km <sup>2</sup> )	Percentage (%)	Area in 2022 (km <sup>2</sup> )	Percent age (%)
1	Natural Vegetation	521,425	39,007	495,954	37,101	456,588	34,156
2	Cultivation Vegetation	772,990	57,826	772,650	57,800	733,560	54,876
3	Open Area	7,130	0,533	29,819	2,231	64,418	4,819
4	Built-in Area	30,774	2,302	33,368	2,496	78,014	5,836
5	Water	4,437	0,332	4,966	0,371	4,176	0,312
	Total	1336,756	100	1336,756	100	1.336, 756	100

#### 3.2.1. Land Cover Transformation between 2014-2018

The construction of the Cipali highway from the end of 2011 to September 2015 (Praditya, 2015) and the development of West Java International Airports in 2014 in Kertajati Districts (Communication and Public Information Bureau of the Ministry of Transportation, 2018) provoke the land cover changes in the northern areas of Majalengka Regency. The land cover transformation was observed between 2014 to 2018, as shown in Table 4. Besides, our data analysis results using the pan-sharpening method and random forest machine learning algorithm from 2014 to 2018 also signified decreasing and increasing land cover area in the Majalengka Regency. The increasing area was observed in the open land, built-up land, and water areas, with the open land scoring the highest increase in area, from originally 130 km<sup>2</sup> in 2014 to 29,819 km<sup>2</sup> in 2018. Linearly, this increase in open land area is followed by the higher built-in area of 33,368 km<sup>2</sup> in 2018 and the water area of 4,966 km<sup>2</sup> in 2018. On the other side, the natural and cultivated vegetation decreased to 495,954 km<sup>2</sup> and 772,650 km<sup>2</sup>, respectively, in 2018.

#### 3.2.2. Land Cover Transformation between 2018-2022

From 2018 to 2022, we also observed the greater area of open land and built-in land areas. The open land area escalated from 29,819 km<sup>2</sup> in 2018 to 64,418 km<sup>2</sup> in 2022. The increase was also observed in the built-in area, from 33,368 km<sup>2</sup> in 2018 to 78,014 km<sup>2</sup> in 2022. Their increase is followed by a decrease of natural vegetation, cultivated, and water areas into 456,588 km<sup>2</sup>, 733,560 km<sup>2</sup>, dan 4,176 km<sup>2</sup>, respectively, in 2022.

The West Java International Airport was inaugurated in 2018, affecting the transformation of the land cover area in the Majalengka Regency. Beginning from its formal opening in 2018 (Communication and Public Information Bureau of the Ministry of Transportation, 2018), there has been an increasing built-in land cover area until 2022.

### 3.2.3. Dynamics of Land Cover Transformation between 2014-2022

From 2014 to 2022, there have been changes in land cover in the Majalengka Regency. As illustrated in Figure 5, the total natural and cultivated land area decrease between 2018 and 2022. Simultaneously, the open land and built-in land area increased between 2018 to 2022. Meanwhile, the water area increased in 2018 and decreased in 2022.

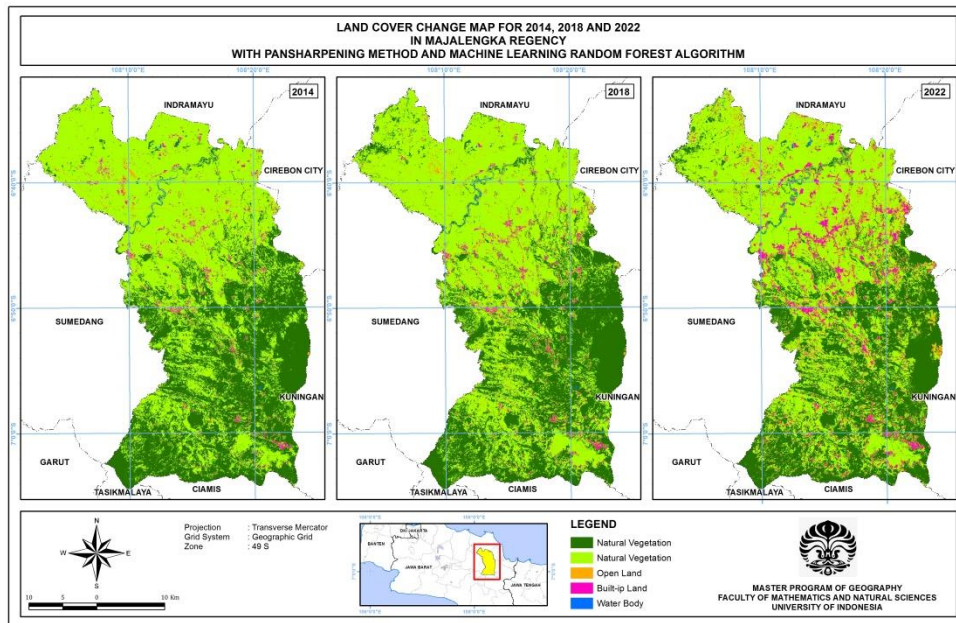


**Figure 5. Map of Land Cover Transformation of Majalengka Regency in 2014, 2018, and 2022**

Spatially, the trend of decreasing vegetation area was observed in the central and southern regions of the Majalengka Regency. The eastern area of Majalengka Regency is a mountainous and undulating or hilly area, with Ceremai Mountain in its south area and Ciwaru Mountain in its southwest area. The decrease in natural vegetation area from 2014 to 2022 is induced by the land clearing for the built-in or cultivated vegetation areas. The same shrinkage trend is also found in the vegetation land area of the central areas of Majalengka Regency. This decrease is caused by the increasing need for housing areas and other buildings for people's economic activities and public activities. As reported in a previous study, the change in land cover may be induced by the activities involving dynamic relationships between humans and the environment (Bintarto, 1977). Besides, the utilization of natural resources and land area also results in the conversion or change in land usage (Akhmaddhian & Vikriandi, 2020). Nuraeni, Sitorus, and Panuju (2017) uncovered that the rapid progression of an area or its population growth causes a land transformation from agricultural to built-in land areas.

In addition, we identified an increase in open and built-in land areas, particularly in the central and some northern areas of the Makaleng Regency. The greater built-in area in the central and northern areas follows the establishment of industrial areas within the regional spatial plan of the Majalengka Regency (Paramasatya & Rudiarto, 2020). Besides, the increase of open land and the built-in area is also inseparable from the enactment of Regional Regulation No 22 the Year 2010, concerning the spatial plan of West Java 2009-2029 and Regional

Regulation No 11 the Year 2011 on the spatial plan of Majalengka Regency. These two laws regulate the construction of West Java International Airports and aerocity areas in the Majalengka Regency. In specific, the West Java International Airport was developed in the Kertajati District, in the northern region of Majalengka Regency. The construction of this international airport and aerocity area was expected to present positive influences on the economy of Majalengka Regency (Rochman, Meilina, Fajriati, Amalia, & Subhan, 2021). Following these regulations, a commitment to maintaining the open land and built-in areas is necessary due to the continuously increasing built-in regions because of the population growth and economic exercises (Namara, Hartono, Latief, & Moersidik, 2022). The spatial and land cover transformation in the Majalengka Regency is shown in Figures 5 and 6.

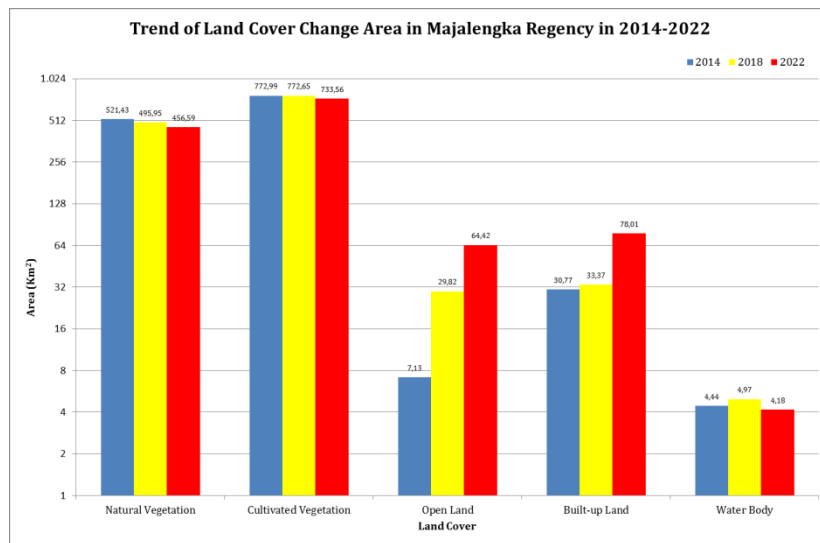


**Figure 6. Transformation of land Cover Area in Majalengka Regency**

In the water area strata, we observed both increasing and decreasing trends. The increase in water area was found from 2014 to 2018, from 0.348 to 0.386% toward the total area of Majalengka Regency. Meanwhile, the decrease was identified from 2018 to 2022, from 0.386 to 0.322% toward the total area of the Majalengka Regency. However, this dynamic of water area transformation is not significant, with slight changes between 2014 to 2022.

### **3.3. The Superiority of Pan-Sharpener Method and Random Forest Machine Learning Algorithm**

Through the pan-sharpening method, we enhanced the spatial resolution of the Landsat 8 images from previously 30 meters to 15 meters. With this more excellent spatial resolution, we can conduct land cover classification in a more detailed manner with better capacity in differentiating the objects within the images, in comparison to the analysis on the multispectral band with 30 meters of resolution. Additionally, the accuracy is also improved since the pan sharpening image results can present a new class of land cover classification, namely the road, as presented in Figure 7. Further, the pan-sharpening method also facilitates apparent differences between buildings and roads (Amini et al., 2022). Then, the pan-sharpening process also aids the land cover classification analysis, especially for the analysis of the urban area that requires satellite images in high resolution (Putra & Setiawan, 2021).

For the random forest machine learning algorithm on the GEE platform, it helps a more rapid land cover classification since it's no longer need computers with high specifications. The multi-temporal land-cover mapping can be carried out using satellite images in the GEE platform and machine learning algorithms (Farda, 2017). Besides, the use of random forest machine learning algorithms in the land cover classification is effective in overcoming the overfitting issues in the land cover classification results (Zulfajri et al., 2021). It is caused by the random mapping of land cover produced by the random forest machine learning algorithm (Marlina, 2022).

**True Color Composite Without Pansharpening  
In the West Java International Airport Area**



**(a). Spatial Resolution 30 meters**

**True Color Composite With Pansharpening In  
the West Java International Airport Area**



**(b). Spatial Resolution 15 meters**

**Figure 7. a) Comparison of True Color Composite Images without Pan-Sharpener, b) the Composite Image with Pan-Sharpener**

#### **4. Conclusion**

From 2014 to 2022, there has been a land cover dynamic in Majalengka Regency. We observed an extensive increase in the open and built-in land classes, with 0.533, 2.231, and 4.819% increases in open land in 2014, 2018, and 2022, respectively. Meanwhile, for the built-in area, we discovered a 2.302, 2.496, and 5.836% increase in 2014, 2018, and 2022, respectively. In contrast, the natural vegetation and cultivated vegetation decreased in the same years. The decrease in natural vegetation in 2014, 2018, and 2022 was 39.007, 37.101, and 34.146%, respectively, while, for the same years, the decrease in cultivated vegetation areas was 57.826, 57.800, and 54.876%. The water area increased from 0.332 to 0.371% in 2018, then decreased to 0.312% in 2022. Additionally, the adoption of the pan-sharpening method produces images with a more detailed presentation, offering better and more detailed land usage classes due to the higher spatial resolution of the obtained images. The use of a random forest machine learning algorithm also aids us generated land cover classification with excellent overall accuracy and kappa index (above 85%). With the obtained accuracy score, the land cover classification produced in this study can be classified as feasible and can be used for the land cover change analysis.

#### **Acknowledgments**

We would like to thank the support from numerous parties for the completion of this research, particularly the National Research and Innovation Agency and the Geography Masters Study Program of Universitas Indonesia. We also would like to address our most

sincere gratitude to the National Welfare Agency and Politics, as well as the Regional Development Agency for Research and Development of Majalengka Regency, for their permission for our data collection process.

## References

- Akhmaddhian, S., & Vikriandi, I. (2020). Perubahan fungsi lahan pertanian menjadi perumahan dan dampaknya terhadap sosial ekonomi masyarakat. *Logika: Jurnal Penelitian Universitas Kuningan*, 11(01), 52–57.
- Amini, S., Saber, M., Rabiei-Dastjerdi, H., & Homayouni, S. (2022). Urban land use and land cover change analysis using random forest classification of landsat time series. *Remote Sensing*, 14(11), 2654.
- Andriany, D. I., & Chofyan, I. (2016). Identifikasi perkembangan lahan sawah dan permukiman di Kabupaten Majalengka. *Prosiding Perencanaan Wilayah dan Kota*, 394–398.
- Awaliyan, R., & Sulistyoadi, Y. B. (2018). Klasifikasi penutupan lahan pada citra satelit Sentinel-2a dengan metode tree algorithm. *ULIN: Jurnal Hutan Tropis*, 2(2), 98–104.
- Bhisma, M. (1997). *Prinsip dan metode riset epidemiologi*. Gajah Mada University Press.
- Bintarto, R. (1977). *Geografi kota*. Yogyakarta: UP. Spring.
- BSN. (2014). *Klasifikasi penutup lahan-bagian 1: Skala kecil dan menengah*. SNI (Standar Nasional Indonesia).
- Central Bureau of Statistics. (2020). *Jumlah penduduk hasil SP2020 menurut wilayah dan jenis kelamin (orang), 2020*. Retrieved from <https://www.bps.go.id/indicator/12/2131/1/jumlah-penduduk-hasil-sp2020-menurut-wilayah-dan-jenis-kelamin.html>
- Communication and Public Information Bureau of the Ministry of Transportation. (2018). *Ragam fakta bandar udara internasional Jawa Barat*. Retrieved from <https://dephub.go.id/post/read/ragam-fakta-bandar-udara-internasional-jawa-barat>
- Farda, N. M. (2017). Multi-temporal land use mapping of coastal wetlands area using machine learning in Google earth engine. *IOP Conference Series: Earth and Environmental Science*, 98(1), 12042. IOP Publishing.
- Fari, T. R. (2017). Pengaruh pansharpening terhadap indeks lahan terbangun ndbi menggunakan citra satelit landsat 8 di kota pontianak. *Seminar Nasional Penginderaan Jauh 2017*.
- Fariz, T. R., Daeni, F., & Sultan, H. (2021). Pemetaan perubahan penutup lahan di Sub-DAS Kreo menggunakan machine learning pada Google Earth Engine. *Jurnal Sumberdaya Alam dan Lingkungan*, 8(2), 85–92.
- Fikri, A. S., Setiawan, F., Violando, W. A., Muttaqin, A. D., & Rahmawan, F. (2021). Analisis perubahan penutupan lahan menggunakan Google Earth Engine dengan Algoritma Cart (studi kasus: Wilayah pesisir Kabupaten Lamongan, Provinsi Jawa Timur). *Prosiding Forum Ilmiah Tahunan (FIT)-Ikatan Surveyor Indonesia (ISI)*, 1, 89–99. Departemen Teknik Geodesi, Fakultas Teknik, Universitas Diponegoro.
- Google Developers. (2021). *Supervised classification*. Retrieved from <https://developers.google.com/earth-engine/guides/classification>
- Hidayati, I. N., Susanti, E., & Utami, W. (2017). Analisis pan-sharpening untuk meningkatkan kualitas spasial citra penginderaan jauh dalam klasifikasi tata guna tanah. *BHUMI: Jurnal Agraria dan Pertanahan*, 3(1), 122–135.
- Horning, N. (2010). Random forests: An algorithm for image classification and generation of continuous fields data sets. *Proceedings of the International Conference on Geoinformatics for Spatial Infrastructure Development in Earth and Allied Sciences, Osaka, Japan*, 911, 1–6.
- Huang, Y., Chen, Z., Tao, Y. U., Huang, X., & Gu, X. (2018). Agricultural remote sensing big data: Management and applications. *Journal of Integrative Agriculture*, 17(9), 1915–1931.
- Koehrsen, W. (2017). *Random forest simple explanation*. Retrieved from <https://williamkoehrsen.medium.com/random-forest-simple-explanation-377895a60d2d>
- Kshetri, T. (2018). Ndvi, ndbi & ndwi calculation using landsat 7, 8. *GeoWorld*, 2, 32–34.
- Marlina, D. (2022). Klasifikasi Tutupan Lahan pada Citra Sentinel-2 Kabupaten Kuningan dengan NDVI dan Algoritme Random Forest. *STRING (Satuan Tulisan Riset dan Inovasi Teknologi)*, 7(1), 41–49.

**Jurnal Pendidikan Geografi:  
Kajian, Teori, dan Praktik dalam Bidang Pendidikan dan Ilmu Geografi**

28(2), 2023, 178-192

- Namara, I., Hartono, D. M., Latief, Y., & Moersidik, S. S. (2022). Policy development of river water quality governance toward land use dynamics through a risk management approach. *Journal of Ecological Engineering*, 23(2), 25–33.
- NASA. (2013). *Landsat 8*. Retrieved from <https://landsat.gsfc.nasa.gov/satellites/landsat-8/landsat-8-bands/>
- Nugroho, J. T. (2013). Identification of inundated area using Normalized Difference Water Index (NDWI) on lowland region of Java island. *International Journal of Remote Sensing and Earth Sciences (IJReSES)*, 10(2), 114–121.
- Nuraeni, R., Sitorus, S. R. P., & Panuju, D. R. (2017). Analisis perubahan penggunaan lahan dan arahan penggunaan lahan wilayah di Kabupaten Bandung. *Buletin Tanah dan Lahan*, 1(1), 79–85.
- Paramasatya, A., & Rudiarto, I. (2020). Implikasi penetapan wilayah pusat pertumbuhan industri terhadap penggunaan lahan di Kabupaten Majalengka. *Jurnal Pembangunan Wilayah dan Kota*, 16(2), 144–157.
- Pradipta, I. M. D., Widyantara, I. M. O., & Hartati, R. S. (2019). Penajaman Citra Satelit Landsat 8 menggunakan Transformasi Brovey. *Majalah Ilmiah Teknologi Elektro*, 18(3), 353–360.
- Praditya, I. I. (2015). *Perjalanan pembangunan Tol Cipali melewati 6 era kepemimpinan RI*. Retrieved from <https://www.liputan6.com/bisnis/read/2254656/perjalanan-pembangunan-tol-cipali-melewati-6-era-kepemimpinan-ri>
- Prayogo, L. M. (2021). Platform Google Earth Engine untuk pemetaan suhu permukaan daratan dari data series modis. *DoubleClick: Journal of Computer and Information Technology*, 5(1), 25–31.
- Putra, I. K. A., & Setiawan, I. M. D. (2021). Aplikasi teknik fusi dengan metode pansharpening untuk analisis penggunaan lahan pada wilayah Bali Selatan. *Media Komunikasi Geografi*, 22(1), 62–74.
- Rochman, B. T. F., Meilina, C., Fajriati, C. E., Amalia, D. N., & Subhan, H. (2021). Analisis ekologi administrasi: Dampak pembangunan Bandara Internasional Jawa Barat (BIJB) Kertajati di Desa Putridalem Kecamatan Jatitujuh Kabupaten Majalengka. *Jurnal Inovasi Penelitian*, 1(12), 2761–2768.
- Sampurno, R. M., & Thoriq, A. (2016). Klasifikasi tutupan lahan menggunakan citra landsat 8 Operational Land Imager (OLI) di Kabupaten Sumedang (land cover classification using landsat 8 Operational Land Imager (OLI) data in Sumedang Regency). *Jurnal Teknotan*, 10(2), 1067–1978.
- Santoso, H., Tani, H., & Wang, X. (2017). Random forest classification model of basal stem rot disease caused by *Ganoderma boninense* in oil palm plantations. *International Journal of Remote Sensing*, 38(16), 4683–4699.
- Tambajong, J., Mononimbar, W., & Lahamendu, V. (2017). Identifikasi perubahan penggunaan lahan koridor jalan trans Sulawesi di Amurang. *SPASIAL*, 4(3), 9–19.
- The Ministry of Communication and Informatics of Majalengka. (2023). *Profil Majalengka*. Retrieved from <https://majalengkakab.go.id/profil-majalengka-2/>
- Wang, L., Wang, J., & Qin, F. (2021). Feature fusion approach for temporal land use mapping in complex agricultural areas. *Remote Sensing*, 13(13), 2517.
- Wiweka, P. E., Prayogo, T., Marini, Y., & Budiman, S. (2014). Uji akurasi training sample untuk klasifikasi terawasi data penginderaan jauh resolusi menengah. *Semin Nas IDEC 2014*, 559–566.
- Zulfajri, Z., Danoedoro, P., & Murti, S. H. (2021). Klasifikasi tutupan lahan data landsat-8 OLI menggunakan metode random forest. *Jurnal Penginderaan Jauh Indonesia*, 3(1), 1–7.
- Zurqani, H. A., Post, C. J., Mikhailova, E. A., Ozalas, K., & Allen, J. S. (2019). Geospatial analysis of flooding from hurricane Florence in the coastal South Carolina using Google Earth Engine. *International Journal of Applied Earth Observation and Geoinformation*, 69, 175–185.